3

Assessment of Neuroinflammation in Transferred EAE Via a Translocator Protein Ligand

F. Mattner et al.*
[1]*Life Sciences Division, Australian Nuclear Science and Technology Organisation Australia*

1. Introduction

Neuroinflammation is involved in the pathogenesis and progression of neurological disorders such as Alzheimer's disease and multiple sclerosis (MS) (Doorduin et al., 2008). MS has been considered a T cell-mediated autoimmune disorder of the central nervous system (CNS), characterized by inflammatory cell infiltration and myelin destruction (Hauser et al., 1986) and focal demyelinated lesions in the white matter are the traditional hallmarks of MS. However more recent evidence suggests more widespread damage to the brain and spinal cord, to areas of white matter distant from the inflammatory lesions and demyelination of deep and cortical grey matter (McFarland & Martin, 2007). Experimental autoimmune encephalomyelitis (EAE) is an extensively used model of T-cell mediated CNS inflammation; modelling disease processes involved in MS. EAE can be induced in several species by immunization with myelin antigens or via adoptive transfer of myelin-reactive T cells. The models of EAE in rodents [actively induced and transferred] provide information about different phases [inflammation, demyelination and remyelination] and types [monophasic, chronic-relapsing and chronic-progressive] of the human disease multiple sclerosis and a vast amount of clinical and histopathologic data has been accumulated through the decades. A key aim of current investigations is developing the ability to recognise the early symptoms of the disease and to follow its course and response to treatment.

Molecular imaging is a rapidly evolving field of research that involves the evaluation of biochemical and physiological processes utilising specific, radioactive, fluorescent and magnetic resonance imaging probes. However, it is positron emission tomography (PET) and single photon emission computer tomography (SPECT) which, due to their exquisite sensitivity involving specifically designed radiolabelled molecules, that is leading the way in molecular imaging and has greatly enabled the non-invasive "visualisation" of many diseases in both animal models and humans. Furthermore, PET and SPECT molecular

* M. Staykova[2], P. Callaghan[1], P. Berghofer[1], P. Ballantyne[1], M.C. Gregoire[1], S. Fordham[2], T. Pham[1], G. Rahardjo[1], T. Jackson[1], D. Linares[2] and A. Katsifis[1]
[1]*Life Sciences Division, Australian Nuclear Science and Technology Organisation, Australia*
[2]*Neurosciences Research Unit, The Canberra Hospita, Australia*

imaging are providing invaluable imaging data based on a biochemical-molecular biology interaction rather than from the traditional anatomical view. Increasingly, PET and SPECT radiotracers have been exploited to study or identify molecular biomarkers of disease, monitor disease progression, determining the effects of a drug on a particular pathology and assess the pharmacokinetic behaviour of pharmaceuticals *in vivo*. Significantly, these new imaging systems provide investigators with an unprecedented ability to examine and measure *in vivo* biological and pharmacological processes over time in the same animals thus reducing experimental variability, time and costs. Molecular imaging based on the radiotracer principle allows chemical processes ranging from cellular events, to cellular communication and interaction in their environment, to the organisation and function of complete tissue and organs to be studied in real time without perturbation. One of the key benefits of molecular imaging is a technique that allows longitudinal studies vital for monitoring intra-individual progression in disease, or regression with supplementary pharmacotherapies. This is key in animal models of diseases such as MS, where there is significant intra-individual variability in the disease course and severity.

Recent investigations have proposed the translocator protein (TSPO; 18 kDa), also known as the peripheral benzodiazepine receptor (PBR), as a molecular target for imaging neuroinflammation (Chen & Guilarte, 2008; Doorduin et al., 2008; Papadopoulos et al., 2006). TSPO (18 kDa) is a multimeric protein consisting of five transmembrane helices, which, in association with a 32 kDa subunit that functions as a voltage dependent anion channel and a 30 kDa subunit that functions as an adenine nucleotide carrier forms part of a hetero-oligomeric complex (McEnery et al., 1992) responsible for cholesterol, heme and calcium transport in specific tissue. TSPO is primarily located on the outer mitochondrial membrane and is predominantly expressed in visceral organs (kidney, heart) and the steroid hormone producing cells of the adrenal cortex, testis and ovaries. In the central nervous system (CNS), TSPO is sparsely expressed under normal physiological conditions, however its expression is significantly upregulated following CNS injury (Chen et al., 2004; Papadopoulos et al., 1997; Venneti et al., 2006; Venneti, et al., 2008).

Several studies have identified activated glial cells as the cells responsible for TSPO upregulation in inflamed brain tissue, both in humans and in experimental models (Mattner et al., 2011; Myers et al., 1991a; Stephenson et al., 1995; Vowinckel et al., 1997) and the TSPO ligand [^{11}C]-PK11195 was one of the first PET ligands used for imaging activated microglia in various neurodegenerative diseases (Venneti et al., 2006). Although [^{11}C]-(R)-PK11195 is widely used for imaging of microglia, its considerable high plasma protein binding, high levels of nonspecific binding, relatively poor blood–brain barrier permeability and short half-life, limits its use in brain imaging (Chauveau et al., 2008). Recently, alternative PET radioligands for TSPO including the phenoxyarylacetamide derivative [^{11}C]-DAA1106 and its analogues (Gulyas et al., 2009; Takano et al., 2010; Venneti et al., 2008), the imidazopyridines (PBR111) and its analogues (Boutin et al., 2007a; Fookes et al., 2008) and the pyrazolo[1,5-a]pyrimidine derivatives [^{18}F]-DPA-714 and [^{11}C]-DPA-713 (Boutin et al., 2007b; James et al., 2008) have been investigated.

In addition to imaging with PET, recent advances in new generation of hybrid SPECT imaging systems enabling increased resolution and morphological documentation with associated computed tomography have been made for use clinically and preclinically. These

advances have created a need and an opportunity for SPECT tracers; particularly those incorporating the longer lived radiotracer iodine-123 (t ½ = 13.2 h), to facilitate extended longitudinal imaging studies.

In this study the recently developed high-affinity TSPO, SPECT ligand, 6-chloro-2-(4'-iodophenyl)-3-(N,N-diethyl)-imidazo[1,2-a]pyridine-3-acetamide or CLINDE , was used to explore the expression of activated glia in a model of transferred EAE (tEAE). [^{123}I]-CLINDE has demonstrated its potency and specificity for TSPO binding, its ability to penetrate the blood-brain barrier and suitable pharmacokinetics for SPECT imaging studies (Mattner et al., 2008). It has also been shown that [^{123}I]-CLINDE was able to detect *in vivo* inflammatory processes characterized by increased density of TSPO in several animal models (Arlicot et al., 2008; Arlicot et al., 2010; Mattner et al., 2005; Mattner et al., 2011; Song et al., 2010), thus representing a promising SPECT radiotracer for imaging neuroinflammation. The present study aimed to investigate the effectiveness of [^{123}I]-CLINDE to detect and quantify the activated glia and consequently correlate the intensity of TSPO upregulation with the severity of disease in a model of tEAE.

2. *In vivo* distribution and *in vitro* binding of TSPO - correlation with upregulation in a model of tEAE

2.1 *In vivo* evaluation

The effectiveness of [^{123}I]-CLINDE to detect and quantify activated glia and correlate TSPO upregulation to the severity of neuroinflammation was assessed on a Lewis rat model of tEAE (Willenborg et al., 1986). The intravenous injection of myelin basic protein (MBP)-specific T lymphoblasts results in a single disease episode. The cells should be used when encephalitogenic, i.e. in the first three days after MBP re-stimulation of spleen or lymph node cells (from MBP- complete Freund's adjuvant (CFA) primed Lewis rats) or established MBP-specific $CD4^+$ IFNγ producing T line cells (De Mestre et al., 2007). A huge advantage of this model of neuroinflammation is its uniform time course.

Male Lewis rats (Animal Resource Centre, Australia) were maintained and monitored according to Australian laws governing animal experimentation. The rats were immunised with emulsion of bovine MBP and CFA (4 mg/ml Mycobacterium butyricum). On day 10 the popliteal and inguinal lymph nodes were removed and single cell suspensions were incubated with the antigens MBP or PPD (50 μg/ml) for 3 days. MBP and PPD lymphoblasts were isolated on a density gradient (d=1.077), propagated in IL-2 containing medium for 25 h and $3x10^7$ cells were injected via the lateral tail vein into naive Lewis rats. The rats were examined daily and a clinical score assigned according to the accepted scale: 0, asymptomatic; 1, flaccid distal half of the tail; 2, entire tail flaccid; 3, ataxia (difficulty righting). Half values were given when assessment fell between two scores.

The radiotracers [^{123}I]-CLINDE and [^{125}I]-CLINDE were synthesized as previously described (Katsifis et al., 2000) using an improved method, giving rise to high purity and high specific activity product. Briefly the tributyltin precursor (50-100 μg) in acetic acid (200 μL) was treated with a solution of either no carrier added Na^{123}I in 0.02 M NaOH (Australian Radioisotopes and Industrials, Sydney, Australia) or Na^{125}I (GE-Healthcare) followed by peracetic acid (1-3%, 100 μL). After 5 min the reaction was quenched (sodium bisulphite, 200 μL, 50 mg/mL), neutralised (sodium bicarbonate, 200 μl, 50 mg/mL) and injected onto a

semipreparative C-18 RP-HPLC column. The purification and isolation of [$^{123/125}$I]-CLINDE was carried out by C-18 RP-HPLC using a mixture of acetonitrile/0.1 M ammonium acetate 55:45 at a flow rate of 4 mL/min. Under these conditions, the radiotracer eluted at 25 min. The eluted product was evaporated to dryness and reconstituted in saline (0.9%) for *in vivo* pharmacological studies. For *in vitro* assays, unlabelled CLINDE was added to the [^{125}I]-CLINDE to achieve a specific activity of 3.7 GBq/μmol and reconstituted in ethanol. The specific activity of [^{123}I]-CLINDE was assumed to be greater than 185 GBq/μmol based on the limit of detection of the UV in the HPLC system used. The specific activity of [^{125}I]-CLINDE was measured as 80 GBq/μmol, close to the theoretical specific activity of the [^{125}I]-iodine.

In order to assess the distribution of the [^{123}I]-CLINDE *in vivo*, rats showing different tEAE clinical scores were used: [0 (pre-clinical, n = 4), 2 (n = 4), 3 (n = 4) and 0 (after recovery, n = 3)]. Rats were given PPD-lymphoblasts (n = 4) and control naive rats (n = 4) served as controls. The animals were injected via the tail vein with 0.70 MBq of [^{123}I]-CLINDE in saline. Tissue samples were taken 3 h later, the radioactivity was measured with an automated gamma counter and the percent injected dose (%ID/g) was calculated by comparison with samples of standard dilutions of the initial dose.

Statistically significant increase in [^{123}I]-CLINDE uptake was measured in brains and spinal cords of Lewis rats given MBP-specific T lymphoblasts that developed EAE with clinical scores of 2 and 3 (Figure 1). In the brain, the medulla oblongata, medulla pons, cerebellum, diencephalon, hypothalamus, hippocampus, frontal and posterior cortex were affected and the increase in [^{123}I]-CLINDE uptake was in the range of 1.5 – 3.8 times.

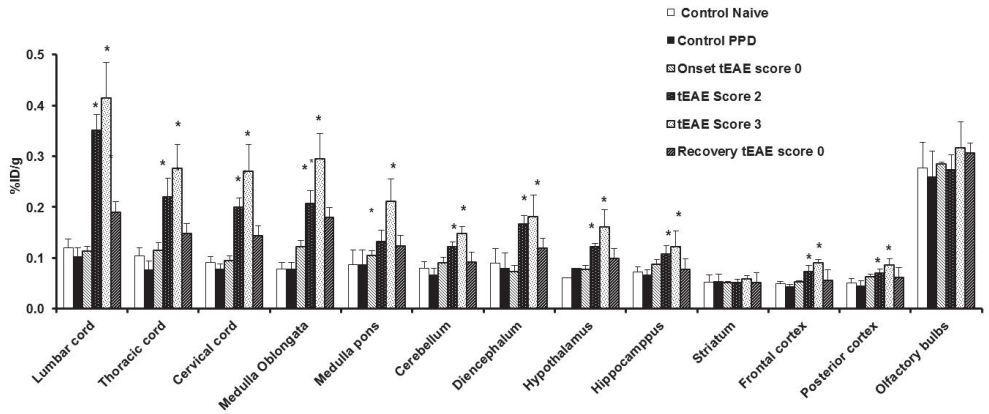

Fig. 1. Uptake of [^{123}I]-CLINDE in the CNS. Data are represented as mean ± SD of wet tissue.* $p<0.05$ - One way ANOVA with Tukeys post-hoc test.

In the spinal cord the uptake of activity reflected the ascending nature of the inflammatory process: lumbar spinal cord > thoracic spinal cord > cervical spinal cord. The positive correlation between the ligand uptake and the disease severity is shown also in Figure 2.

Importantly, the radiotracer uptake on day 4 did not differ significantly from the one in the naive controls if the disease irrelevant PPD-specific T lymphoblasts or the disease relevant

MBP-specific T lymphoblasts were injected (Figure 1). Also, all animals showed the typical TSPO ligand biodistribution in the visceral organs and EAE severity had no influence on ligand uptake in the visceral organs (Table 1).

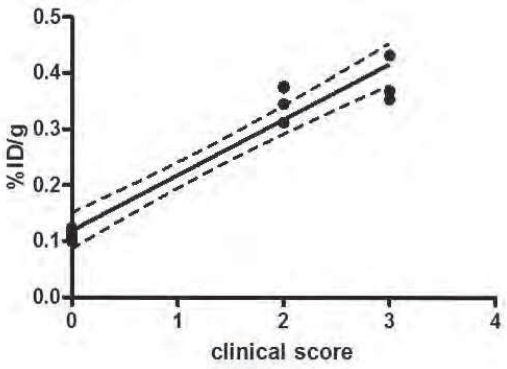

Fig. 2. Correlation between uptake of [123I]-CLINDE and disease severity in the lumbar spinal cord. Linear regression analysis, r squared value (0.97) and error bars being 95% confidence intervals for fit.

Organ	Control		tEAE			
	Naive n = 4	PDD n = 4	Score 0 Preclinical n = 4	Score 2 n = 4	Score 3 n = 4	Score 0 recovery n = 4
Liver	0.27±0.05	0.27±0.03	0.32±0.03	0.32±0.03	0.33±0.02	0.25±0.03
Spleen	3.01±0.45	3.12±0.34	3.49±0.10	3.14±0.32	3.24±0.37	3.33±0.49
Kidney	2.07±0.36	1.68±0.07	2.24±0.11	2.03±0.13	2.33±0.37	1.97±0.25
Lungs	2.27±0.41	2.01±0.18	2.41±0.32	2.12±0.16	2.27±0.38	2.05±0.24
Heart	3.24±0.49	2.85±0.29	3.81±0.14	2.87±0.08	3.16±0.31	3.32±0.03
Blood	0.04±0.01	0.04±0.01	0.06±0.00	0.04±0.01	0.05±0.01	0.04±0.00
Pancreas	0.61±0.12	0.51±0.04	0.64±0.06	0.58±0.07	0.62±0.05	0.55±0.08
Thymus	0.84±0.09	0.81±0.34	1.17±0.26	0.85±0.24	1.33±0.34	1.12±0.23
Adrenals	7.69±1.27	6.38±0.62	7.86±0.37	7.00±0.93	7.22±1.33	8.49±2.10

Table 1. Biodistribution of [123I]-CLINDE in the visceral organs of Lewis rats given MBP-specific T lymphoblasts and controls**.** Results are expressed as %ID/g ± SD of wet tissue

The specificity of [123I]-CLINDE binding was demonstrated in a competition study with the PK11195 (Sigma-RBI) injected in rats with tEAE clinical score 2. The *in vivo* specificity of [123I]-CLINDE was tested in two groups of four rats with tEAE clinical score 2 by injecting only [123I]-CLINDE or by injecting PK11195 (5 mg/kg) prior to [123I]-CLINDE. PK11195 was dissolved in saline with 5% dimethyl sulfoxide and injected 5 minutes prior to the injection of 0.70 MBq of the radiotracer. Animals were sacrificed 3 h p.i. and the tissues were analysed as described above.

Administration of PK11195 reduced the uptake of [123I]-CLINDE in the CNS (Figure 3) and the visceral organs with TSPO expression (data not shown) by 65-85% confirming the specificity of the ligand.

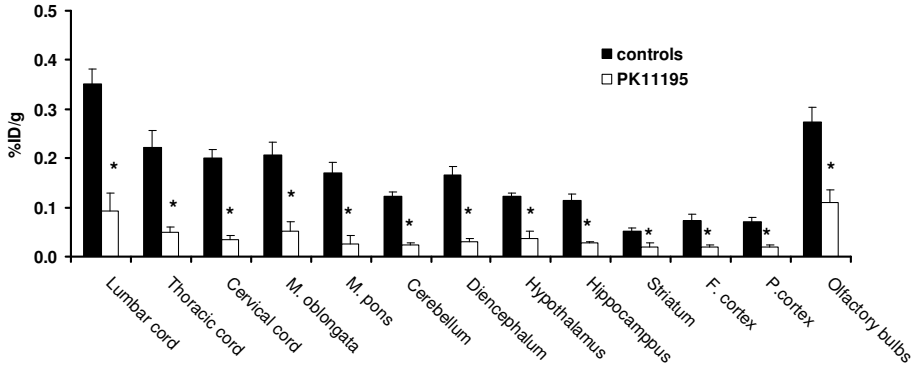

Fig. 3. Specificity of [123I]-CLINDE binding in CNS. Data are represented as mean ± SD.
* $p<0.05$ - Mann Whitney test

The feasibility of using TSPO as a marker to assess the degree of microglia activation in the living rat was tested using [123I]-CLINDE on a dedicated small animal SPECT imaging system. Longitudinal imaging studies were performed using a small animal dual-head SPECT/CT camera (Flex X-SPECT, Gamma Medica Ideas Inc.) equipped with 1 mm-aperture pinhole collimators (McElroy et al., 2002). Four rats given MBP-specific T lymphoblasts and 2 control naive animals were used. The experimental rats were imaged four times (baseline, day 4, 6 and 11 post tEAE induction), while controls were imaged twice on alternate days.

Rats were injected via the tail vein with [123I]-CLINDE (20-30 MBq in 0.1 ml saline) and anaesthetized with isoflurane (2.5%). Their heads were carefully positioned at the centre of the field-of-view, and scanned between 40 and 104 minutes after the radiotracer injection. Sixty-four 1 min-projections were collected over 360 degrees by each head, at a radius-of-rotation of 45 mm. CT scan of the rat head was then performed in order to provide anatomical landmarks for the analysis. The SPECT projections of the two heads were combined and reconstructed with an iterative cone-beam algorithm (16 subsets, 4 iterations). The reconstructed data were then scaled using calibration factors to allow the measured activity to be expressed as %ID/mL. SPECT and CT volumes were automatically fused for each of the eight scans. All CT volumes of the same rat were then manually co-registered to the first one (reference), using an image visualisation and processing software (http://brainvisa.info). A rat brain atlas was finally coregistered onto the reference volume and statistics derived for each Region of Interest.

The average values of [123I]-CLINDE uptake in the brain measured before the induction of tEAE (expressed as a percentage of injected dose per mL) (0.64 ± 0.1%ID/mL) is equivalent to the average uptake of all controls imaged during the study period (0.71 ± 0.3%ID/mL). The peak increase in activity is reached 6 days post immunization and the uptake depends on the clinical score of the rat. The uptake of [123I]-CLINDE, as assessed by SPECT imaging

during the course of the study, is exemplified in the hypothalamus and midbrain (Fig 4A). The spatial distribution of the activity in the brain of one typical rat over time is shown in figure 4B.

Using this small animal SPECT system we could not find statistically significant differences between intra-cerebral structures in the different groups of animals. This was probably due to the fluctuation of uptake values among animals from the same experimental group showing different tEAE scoring (Figure 4A). Moreover based on the example in Figure 4, the peak uptake in different structures of the brain differs from rat to rat depending on the tEAE score, disease severity, and therefore averaging the values for the experimental group did not reach statistical significance in the data. However the brain structures that showed an increase in uptake by SPECT imaging were the same structures where increased uptake was observed in the biodistribution studies.

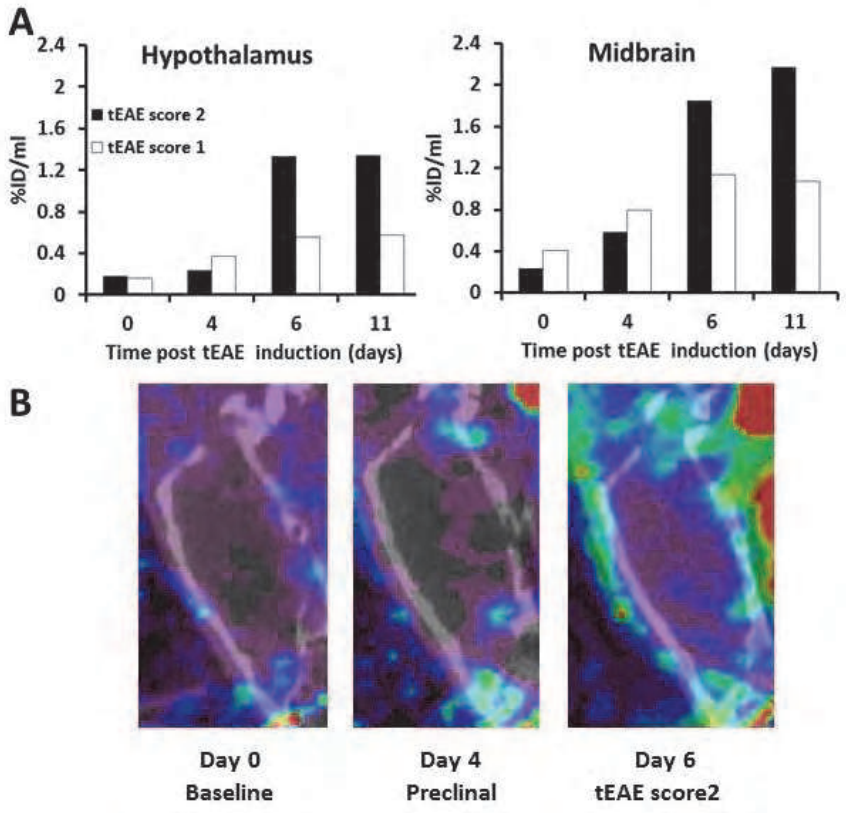

Fig. 4. *In vivo* SPECT imaging of TSPO in brain of rats given MBP-specific T lymphoblasts. **(A)** Representative individual dynamics of [^{123}I]-CLINDE uptake in hypothalamus and midbrain (expressed as a percentage of injected dose per mL). **(B)** Representative SPECT images of [^{123}I]-CLINDE uptake in a rat brain. The SPECT images shown were coregistered with CT at 0 (baseline), 4 and 6 days after induction of tEAE.

2.2 Autoradiography and immunochemistry correlation with the upregulation of TSPO in the tEAE model

In vitro and *ex vivo* autoradiography with [^{125}I]-CLINDE was performed to delineate the CNS areas with TSPO uptake.

For *in vitro* autoradiography, animals with tEAE clinical scores: 2 (n = 3) and 0 (after recovery, n = 5) and 7 control naive rats were used. Brains and spinal cords were frozen in isopentane at -80°C. Coronal sections (20 μm thick) were cut, mounted onto polysine coated slides and stored at -20°C. TSPO receptors were labeled with [^{125}I]-CLINDE (3.7 GBq/μmol) at 3 nM concentration in Tris-HCl, pH 7.4 at 4°C for 60 min. Nonspecific binding was defined by incubating adjacent tissue sections with 10 μM of PK11195. The incubation was terminated by rinsing sections twice for 2 min in cold incubation buffer. Sections were then dipped briefly in cold distilled water and dried rapidly under a stream of cold air. The sections were affixed together with calibration standards (Amersham) to radiographic films (Amersham Hyperfilm-βmax) for 4-6 h and developed using GBX developer and fixer (Kodax). The autoradiograms were analysed using a Microcomputer Imaging Device (MCID, Imaging research, Ontario, Canada).

For *ex vivo* autoradiography rats with tEAE clinical scores: 3 (n = 3) and 0 (after recovery, n = 3) and control naive rats (n = 3) were given [^{125}I]-CLINDE (1.85 MBq in 100 μl of saline) i.v. and were sacrificed 3 h after the injection of the radiotracer. Brains and spinal cords were frozen in isopentane at -80°C. Coronal sections (20 μm thick) were cut, thawed, dried and affixed to radiographic films (Amersham Hyperfilm-βmax) for 10-15 days and the autoradiograms analyzed as above.

In vitro autoradiography with [^{125}I]-CLINDE of the spinal cord from rats with tEAE compared to controls showed statistically significant increased binding of TSPO in areas of the grey (2 times) and white matter (1.2 - 3 times) (Figure 5). This study extends earlier observations using [^{3}H](*R*)-PK11195 (Banati et al., 2000) in which increased binding in the spinal cords from rats with tEAE, at peak of clinical disease was documented.

The *in vitro* and *ex vivo* autoradiography revealed an increase in the TSPO expression at three brain levels (Figure 6), i.e. nuclear diagonal band/rostral migratory stream; substantia nigra cerebral peduncle and mammillary nucleus; ventral cochlear nucleus. Histologically, a lesion was observed in one of the five brains at level -3 mm to bregma, in the region of substantia nigra.

As the autoradiography showed a clear increase in TSPO labelling at specific regions in the forebrain, midbrain and hindbrain as well as in the spinal cord (Figures 5 and 6), immunohistochemistry was also performed in order to clarify the presence of gliosis in the TSPO positive areas.

For this purpose, brains from 2 naive rats, 2 rats given PPD-lymphoblasts (day 4), 4 rats given MBP-lymphoblasts (day 4), 3 rats tEAE score 2 and 3 rats after recovery from the episode, were fixed in formalin, placed in David Kopf Instruments (Tujunga, CA) brain blocker and cut at six levels at a distance of 2 mm. Serial 4 μm coronal paraffin sections were taken at each of the six levels and assessed according to the rat brain atlas of Paxinos and Watson (Paxinos & Watson, 2007).

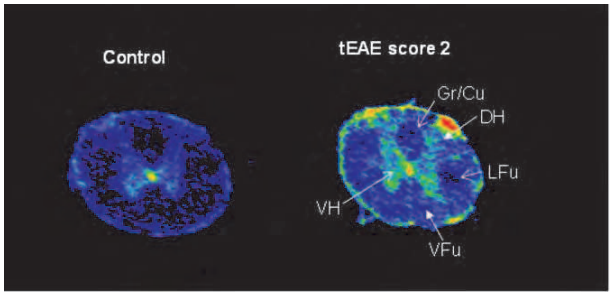

Grey matter	Control	tEAE Score 2	tEAE recovery Score 0
Dorsal horn (DH)	155 ± 17	365 ± 36***	236 72‡
Ventral horn (VH)	225 ± 17	225 ± 30	270 26
White matter			
Lateral funiculus (LFu)	123 ± 10	266 ± 23***	132 ± 31‡‡‡
Ventral funiculus (VFu)	128 ± 14	369 ± 64***	118 ± 18‡‡‡
Gracile/ Cuneate Fasciculus (Gr/Cu)	117 ± 18	228 ± 7**	113 ± 17‡‡

Fig. 5. Different cervical spinal cord TSPO expression in control rats and in rats with tEAE, using *in vitro* [^{125}I]-CLINDE autoradiography. Results are expressed as fmol/mg T.E ± SD, *n* = 3-7, one way ANOVA with Tukeys Post Hoc test (Control vs Score 2, **p<0.01, *** p<0.001; Score 2 vs Recovery, ‡ p<0.05, ‡‡ p<0.01, ‡‡‡ p<0.001)

Indeed, at the level of the midbrain, in three of the four rats studied, astrogliosis was found around the lateral ventricles on day 4 after tEAE induction, i.e. just before and at the time of onset of the clinical EAE signs (Figure 7). However, with labelling for GFAP and ED-1 no changes were observed in any of the other five brain levels studied as well as in none of the six levels in three rats with tEAE score 2 and in three rats after recovery from score 2 to score 0.

The autoradiography and immunohistochemistry results confirm the immunofluorescence observations of Meeson et al (Meeson et al., 1994) indicating very little brain inflammation that is localised in the forebrain around the third ventricle. It is tempting to speculate that the change in the medial habenular nucleus and the dentate gyrus gliosis reflects a stress

reaction (Sugama et al., 2002), as this was observed around the onset of tEAE and did not persist during its development.

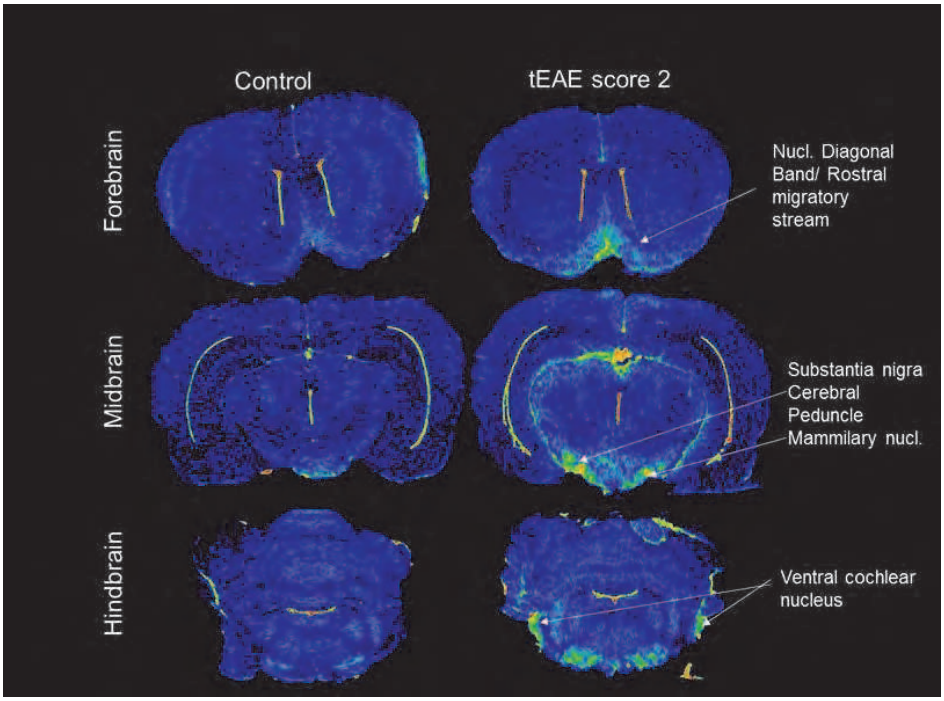

Fig. 6. Brain *in vitro* autoradiography after administration of [^{125}I]-CLINDE in Lewis rats given MBP-specific T lymphoblasts and controls

Longitudinal sections of the spinal cords were examined at the lumbar, thoracic and cervical level. After antigen retrieval (20 min boiling in citrate buffer, pH 6.0) and blocking of endogenous peroxidase and non-specific antibody binding, the macrophage/activated microglial cells were labelled with mouse anti-rat ED-1 biotin-conjugated monoclonal antibody (Serotec); TSPO – with goat polyclonal anti-TSPO IgG (Santa Cruz Biotechnology); the astrocytes - with rabbit anti-GFAP antibody (Sapphire Bioscience) and the chemokine CXCL11 - with rabbit anti-rat I-TAC IgG (kind gift from Prof. Shaun McCall, Chemokine Biology, Department of Molecular Biosciences, Adelaide University). The staining was with InnoGenex IHC Kit (San Ramon, CA) with aminoethyl carbazole (AEC) as peroxidase substrate. The sections were counterstained with Mayer's haematoxylin.

Although the histopathologic analysis and magnetic resonance (MR) microscopy had excellent correlation regarding the extent of white matter lesions on the rat EAE model (Steinbrecher et al., 2005), this imaging technology is not suitable for detection of inflammatory infiltrates in the grey matter. In our experiments significant [^{123}I]-CLINDE uptake was registered in the grey matter of the spinal cord of Lewis rats with tEAE score 2 and 3 (Figure 5). This increased uptake correlated with the positive staining for the chemokine CXCL11 that is produced mainly by astrocytes as well as with the presence of

numerous ED-1 positive cells (macrophages/glial cells) that were visualised in the spinal cord meninges and parenchyma during the tEAE episode (Figure 8). Importantly, some of these activated glial cells were positive for TSPO that supports the autoradiography quantitative data. Two days after spontaneous recovery from tEAE episode, few parenchymal cells were positive for ED-1 and there was no staining for TSPO and the chemokine CXCL11 (I-TAC).

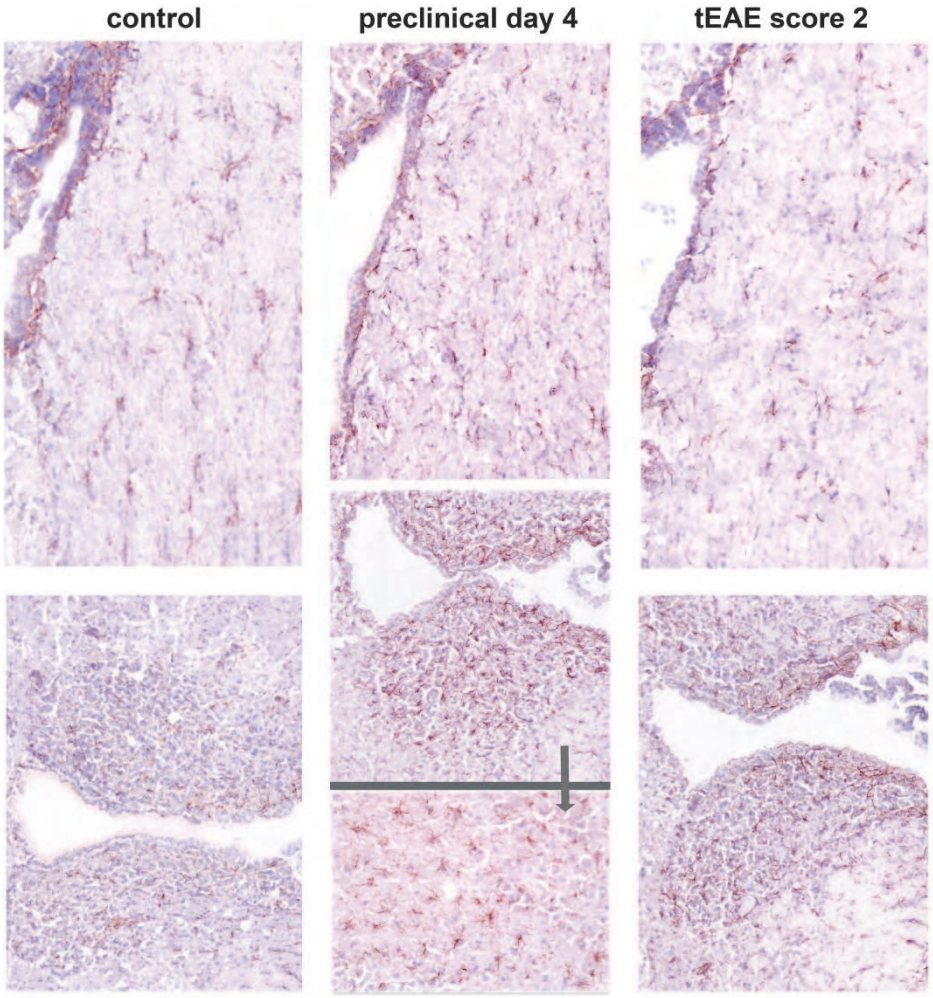

Fig. 7. Glial activation in Lewis rat tEAE (immunohistochemical evaluation). Midbrains labelled for GFAP. At disease onset, astroglyosis was observed around the 3rd ventricle in four of five animals.

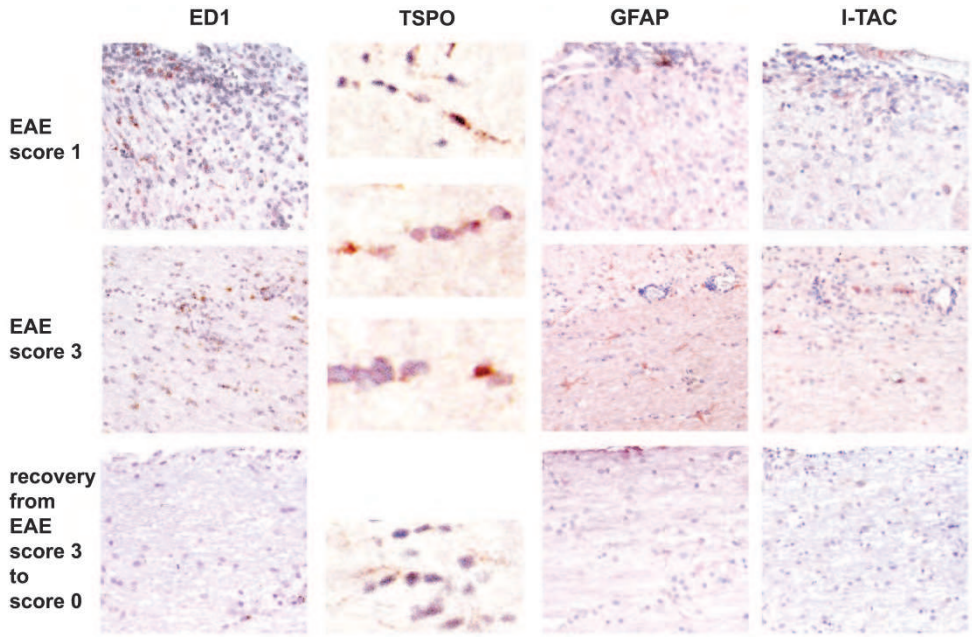

Fig. 8. Longitudinal sections of lumbar spinal cord labelled for macrophages/activated microglia (ED-1), TSPO, astrocytes and I-TAC at different clinical stages of tEAE.

One of the first *in vivo* MRI studies on tEAE in rats (Morrissey et al., 1996) showed that MRI changes were observed well before the onset of major cellular infiltration and before the onset of clinical signs that made possible to assess quantitatively the breach of the blood brain barrier (BBB) and to distinguish *in vivo* between two components of the early phase of the lesion - inflammatory infiltrates and vasogenic oedema. Increased binding of several TSPO ligands has been reported after brain injury, including focal (Myers et al., 1991a; Myers et al., 1991b) and global (Stephenson et al., 1995) cerebral ischemia in the rat where heterogeneous level of expression of TSPO in different cells is seen in the core of infarction as early as 4 days after ischemia (Rojas et al., 2007).

In this model of neuroantigen-specific neuroinflammation the significant changes were also registered from day 4 onward with SPECT imaging. A study on the same model (Banati et al., 2000) also found normal autoradiography up to day 4 with [3H]-PK11195. One should point out that we used two appropriate controls (not only naive rats). Interestingly, the time frame is similar for PET scan studies in stroke patients - the increase in binding was as early as 3 days after the onset of stroke (Price et al., 2006). Thus, any earlier in vivo as well as in vitro changes are most likely attributed to stress reaction.

The imaging studies, using the SPECT tracer [123I]-CLINDE in Lewis rat models of transferred EAE (this study) and active EAE (Mattner et al., 2005) confirm the MRI studies by other groups that the imaging changes parallel the monocyte/microglia/astrocyte activation rather than the lymphocyte infiltration (Morrissey et al., 1996; Rausch et al., 2003). These results confirm the reliability of the translocator protein (Papadopoulos &

Lecanu, 2009) in early diagnostics of antigen-specific neuroinflammation and eventually - of MS.

N.B. Discussion with mouse tEAE models was not included as they result in inflammation which progresses to demyelination (Mokhtarian et al., 1984) while the MBP-specific T lymphoblasts induced tEAE in the Lewis rat is monophasic with full recovery (Holda et al., 1980; Paterson et al., 1981).

3. Conclusion

Transferred EAE was induced in Lewis rats with MBP-specific T lymphoblasts and the uptake of the translocator protein (TSPO) tracer [^{123}I]-CLINDE was studied by biodistribution, *in vitro* and *ex vivo* autoradiography, immunohistochemistry and SPECT imaging. On a background of the typical TSPO ligand biodistribution in the visceral organs, a statistically significant 2-4 fold increase was measured in brains and spinal cords of animals with EAE clinical score of 3, compared to controls (naive or given disease-irrelevant PPD-specific T-lymphoblasts). Importantly, using [^{123}I]-CLINDE as a radiotracer we were able to register significant inflammation also in the grey matter. The CNS regional [^{123}I]-CLINDE uptake correlated with the immunohistochemical localisation of activated glial cells. The results demonstrate the ability of this highly specific TSPO ligand to measure changes in TSPO density according to area of involvement and the severity of disease suggesting it is a useful SPECT tracer for studies on experimentally induced inflammation and in multiple sclerosis.

4. Acknowledgment

The authors sincerely thank Dr David Willenborg, a Visiting Fellow at the ANU Medical School, for his encouragement and advice. M. Staykova is a Visiting Fellow at the John Curtin School of Medical Research, ANU, Canberra, Australia.

5. References

Arlicot, N.; Katsifis, A.; Garreau, L.; Mattner, F.; Vergote, J.; Duval, S.; Kousignian, I.; Bodard, S.; Guilloteau, D. & Chalon, S. (2008). Evaluation of CLINDE as Potent Translocator Protein (18 kDa) SPECT Radiotracer Reflecting the Degree of Neuroinflammation in a Rat Model of Microglial Activation. *European Journal of Nuclear Medicine and Molecular Imaging,* Vol.35, No.12, (December 2008), pp. 2203-2211, ISSN 1619-7089

Arlicot, N.; Petit, E.; Katsifis, A.; Toutain, J.; Divoux, D.; Bodard, S.; Roussel, S.; Guilloteau, D.; Bernaudin, M. & Chalon, S. (2010). Detection and Quantification of Remote Microglial Activation in Rodent Models of Focal Ischaemia Using the TSPO Radioligand CLINDE. *European Journal of Nuclear Medicine and Molecular Imaging,* Vol.37, No.12, (December 2010) pp. 2371-2380, ISSN 1619-708

Banati, R.B.; Newcombe, J.; Gunn, R.N.; Cagnin, A.; Turkheimer, F.; Heppner, F.; Price, G.; Wegner, F.; Giovannoni, G.; Miller, D.H.; Perkin, G.D.; Smith, T.; Hewson, A.K.; Bydder, G.; Kreutzberg, G.W.; Jones, T.; Cuzner, M.L. & Myers, R. (2000). The Peripheral Benzodiazepine Binding Site in the Brain in Multiple Sclerosis -

Quantitative In Vivo Imaging of Microglia as a Measure of Disease Activity. *Brain* Vol.123, (November 2000), pp. 2321-2337 ISSN 0006-8950

Boutin, H.; Chauveau, F.; Thominiaux, C.; Kuhnast, B.; Gregoire, M.C.; Jan, S.; Trebossen, R.; Dolle, F.; Tavitian, B.; Mattner, F. & Katsifis, A. (2007a). In Vivo Imaging of Brain Lesions With [C-11]ClINME, a New PET Radioligand of Peripheral Benzodiazepine Receptors. *Glia,* Vol.55, No.14, (November 2007), pp. 1459-1468, ISSN 0894-1491

Boutin, H.; Chauveau, F.; Thominiaux, C.; Gregoire, M.C.; James, M.L.; Trebossen, R.; Hantraye, P.; Dolle, F.; Tavitian, B. & Kassiou, M. (2007b). C-11-DPA-713: a Novel Peripheral Benzodiazepine Receptor PET Ligand for in Vivo Imaging of Neuroinflammation. *Journal of Nuclear Medicine*, Vol.48, No.4, (April 2007), pp. 573-581, ISSN 0161-5505

Chauveau, F.; Boutin, H.; Van Camp, N.; Dolle, F. & Tavitian, B. (2008). Nuclear Imaging of Neuroinflammation: a Comprehensive Review of [C-11]PK11195 Challengers. *European Journal of Nuclear Medicine and Molecular Imaging,* Vol.35, No.12, (December 2008), pp. 2304-2319, ISSN 1619-7070

Chen, M.K.; Baidoo, K.; Verina, T. & Guilarte, T.R. (2004). Peripheral Benzodiazepine Receptor Imaging in CNS Demyelination: Functional Implications of Anatomical and Cellular Localization. *Brain*, Vol.127, No.6, (July 2004), pp. 1379-1392, ISSN 0006-8950

Chen, M.K. & Guilarte, T.R. (2008). Translocator Protein 18 Kda (TSPO): Molecular Sensor of Brain Injury and Repair. *Pharmacology & Therapeutics*, Vol.118, No.1 (April 2008), pp. 1-17, ISSN 0163-7258

De Mestre, A.M.; Staykova, M.A.; Hornby, J.R.; Willenborg, D.O. & Hulett, M.D. (2007). Expression of the Heparan Sulfate-Degrading Enzyme Heparanase is Induced in Infiltrating CD4+ T Cells in Experimental Autoimmune Encephalomyelitis and Regulated at the Level of Transcription by Early Growth Response Gene 1. *Journal of Leukocyte Biology,* Vol.82, No.5, (November 2007) pp. 1289-1300, ISSN 0741-5400

Doorduin, J.; De Vries, E.F.J.; Dierckx, R.A. & Klein, H.C. (2008). PET Imaging of the Peripheral Benzodiazepine Receptor: Monitoring Disease Progression and Therapy Response in Neurodegenerative Disorders. *Current Pharmaceutical Design*, Vol.14, No.31, (November 2008), pp. 3297-3315, ISSN 1381-6128

Fookes, C.J.; Pham, T.Q.; Mattner, F.; Greguric, I.; Loc'h, C.; Liu, X.; Berghofer, P.; Shepherd, R.; Gregoire, M.C. & Katsifis, A. (2008). Synthesis and Biological Evaluation of Substituted [18F]Imidazo[1,2-a]pyridines and [18F]Pyrazolo[1,5-a]pyrimidines for the Study of the Peripheral Benzodiazepine Receptor Using Positron Emission Tomography. *Journal of Medicinal Chemistry,* Vol.51, No.13, (July 2008), pp. 3700-3712, ISSN 1520-4804

Gulyas, B.; Makkai, B; Kasa, P.; Gulya, K.; Bakota, L.; Varszegi, S.; Beliczai, Z.; Andersson, J.; Csiba, L.; Thiele, A.; Dyrks, T.; Suhara, T.; Suzuki, K.; Higuchi, M. & Halldin, C. (2009). A Comparative Autoradiography Study in Post Mortem Whole Hemisphere Human Brain Slices Taken from Alzheimer Patients and Age-Matched Controls Using Two Radiolabelled DAA1106 Analogues With High Affinity to the

Peripheral Benzodiazepine Receptor (PBR) System. *Neurochemistry International,* Vol.54, No.1, (January 2009), pp. 28-36, ISSN 0197-0186

Hauser, S.L.; Bhan, A.K.; Gilles, F.; Kemp, M.; Kerr, C. & Weiner, H.L. (1986). Immunohistochemical Analysis of the Cellular Infiltrate in Multiple Sclerosis Lesions. *Annals of Neurology,* Vol.19, No.6, (June 1986), pp. 578-587, ISSN 0364-5134

Holda, J.H.; Welch, A.M. & Swanborg, R.H. (1980). Autoimmune Effector Cells. I. Transfer of Experimental Encephalomyelitis with Lymphoid Cells Cultured with Antigen. *European Journal of Immunology*, Vol.10, No.8, (August 1980), pp. 657-659, ISSN 0014-2980

James, M.L.; Fulton, R.R.; Vercoullie, J.; Henderson, D.J.; Garreau, L.; Chalon, S.; Dolle, F.; Selleri, S.; Guilloteau, D. & Kassiou, M. (2008). DPA-714, a New Translocator Protein-Specific Ligand: Synthesis, Radiofluorination, and Pharmacologic Characterization. *Journal of Nuclear Medicine*, Vol.49, No.5, (May 2008), pp. 814-822, ISSN 0161-5505

Katsifis, A.; Mattner, F.; Dikic, B. & Papazian, V. (2000). Synthesis of Substituted [123I]Imidazo[1,2-a]pyridines as Potential Probes for the Study of the Peripheral Benzodiazepine Receptors Using SPECT. *Radiochimica Acta,* Vol. 88, No. 3-4, pp. 229-232, ISSN 0033-8230

Mattner, F.; Katsifis, A.; Staykova, M.; Ballantyne, P. & Willenborg, D.O. (2005). Evaluation of a Radiolabelled Peripheral Benzodiazepine Receptor Ligand in the Central Nervous System Inflammation of Experimental Autoimmune Encephalomyelitis: a Possible Probe for Imaging Multiple Sclerosis. *European Journal of Nuclear Medicine and Molecular Imaging,* Vol.32, No.5 (May 2005), pp. 557-563, ISSN 1619-7070

Mattner, F.; Mardon, K. & Katsifis, A. (2008). Pharmacological Evaluation of [I-123]-ClINDE: a Radioiodinated Imidazopyridine-3-Acetamide for the Study of Peripheral Benzodiazepine Binding Sites (PBBS). *European Journal of Nuclear Medicine and Molecular Imaging*, Vol.35, No.4, (April 2008), pp. 779-789, ISSN 1619-7070

Mattner, F.; Bandin, D.; Staykova, M.; Berghofer, P.; Gregoire, M.; Ballantyne, P.; Quinlivan, M.; Fordham, S.; Pham, T.; Willenborg, D. & Katsifis, A. (2011). Evaluation of [^{123}I]-CLINDE as a Potent SPECT Radiotracer to Assess the Degree of Astroglia Activation in Cuprizone-Induced Neuroinflammation. *European Journal of Nuclear Medicine and Molecular Imaging,* Vol. 38, No. 8 (August 2011), pp. 1516-1528, ISSN 1619-7070

McElroy, D.P.; MacDonald, L.R.; Beekman, F.J.; Yuchuan, W.; Patt, B.E.; Iwanczyk, J.S.; Tsui, B.M.W. & Hoffman, E.J. (2002). Performance Evaluation of A-SPECT: a High Resolution Desktop Pinhole SPECT System for Imaging Small Animals. *IEEE Transactions on Nuclear Science,* Vol.49, No.5 (May 2002), pp. 2139-2147, ISSN 0018-9499

McEnery, M.W.; Snowman, A.M.; Trifiletti, R.R. & Snyder, S.H. (1992). Isolation of the Mitochondrial Benzodiazepine Receptor: Association with the Voltage-Dependent

Anion Channel and the Adenine Nucleotide Carrier. *Proccedings of the National Academy of Sciences USA,* Vol.89, No.8 (May 1992), pp. 3170-3174, ISSN 0027-8424

McFarland, H.F. & Martin, R. (2007). Multiple sclerosis: a complicated picture of autoimmunity. *Nature Immunology,* Vol.8, No.9, (September 2007), pp. 913-919, ISSN 1529-2908

Meeson, A.P.; Piddlesden, S.; Morgan, B.P. & Reynolds, R. (1994). The Distribution of Inflammatory Demyelinated Lesions in the Central Nervous System of Rats with Antibody-Augmented Demyelinating Experimental Allergic Encephalomyelitis. *Experimental Neurology,* Vol.129, No.2 (October 1994), pp. 299-310, ISSN 0014-4886

Mokhtarian, F.; McFarlin, D.E. & Raine, C.S. (1984). Adoptive Transfer of Myelin Basic Protein-Sensitized T Cells Produces Chronic Relapsing Demyelinating Disease in Mice. *Nature,* Vol.309, No.5966, (May 1984), pp. 356-358, ISSN 0028-0836

Morrissey, S.P.; Stodal, H.; Zettl, U.; Simonis, C.; Jung, S.; Kiefer, R.; Lassmann, H.; Hartung, H.P.; Haase, A. & Toyka, K.V. (1996). In vivo MRI and its Histological Correlates in Acute Adoptive Transfer Experimental Allergic Encephalomyelitis. Quantification of Inflammation and Oedema. *Brain*, Vol.119, No.Pt 1, (February 1996), pp. 239-248, 0006-8950

Myers, R.; Manjil, L.G.; Cullen, B.M.; Price, G.W.; Frackowiak, R.S. & Cremer, J.E. (1991a). Macrophage and Astrocyte Populations in Relation to [3H]PK 11195 Binding in Rat Cerebral Cortex Following a Local Ischaemic Lesion. *Journal of Cerebral Blood Flow Metabolism,* Vol.11, No.2, (March 1991), pp. 314-322, 0271-678X

Myers, R.; Manjil, L.G.; Frackowiak, R.S. & Cremer, J.E. (1991b). [3H]PK 11195 and the Localisation of Secondary Thalamic Lesions Following Focal Ischaemia in Rat Motor Cortex. *Neuroscience Letters,* Vol.133, No.1, (November 1991), pp. 20-24 ISSN 0304-3940

Papadopoulos, V.; Amri, H.; Boujrad, N.; Cascio, C.; Culty, M.; Garnier, M.; Hardwick, M.; Li, H.; Vidic, B.; Brown, A.S.; Reversa, J.L.; Bernassau, J.M. & Drieu, K. (1997). Peripheral Benzodiazepine Receptor in Cholesterol Transport and Steroidogenesis. *Steroids*, Vol.62, No.1, (January 1997), pp. 21-28, ISSN 0039-128X

Papadopoulos, V.; Baraldi, M.; Guilarte, T.R.; Knudsen, T.B.; Lacapere, J.J.; Lindemann, P.; Norenberg, M.D.; Nutt, D.; Weizman, A.; Zhang, M.R. & Gavish, M. (2006). Translocator Protein (18 kDa): New Nomenclature for the Peripheral-Type Benzodiazepine Receptor Based on its Structure and Molecular Function. *Trends in Pharmacological Sciences*, Vol.27, No.8 (August 2006), pp. 402-409, ISSN 0165-6147

Papadopoulos, V. & Lecanu, L. (2009). Translocator Protein (18 kDa) TSPO: an Emerging Therapeutic Target in Neurotrauma. *Experimental Neurology*, Vol.219, No.1 (September 2009), pp. 53-57, ISSN 0014-4886

Paterson, P.Y.; Day, E.D. & Whitacre, C.C. (1981). Neuroimmunologic Diseases: Effector Cell Responses and Immunoregulatory Mechanisms. *Immunology Reviews,* Vol.55, No.1, (January 1981), pp. 89-120, ISSN0105-2896

Paxinos, G. & Watson, C. (2007). *The rat brain in stereotaxic coordinates*. Elsevier Academic Press, 6th Edition, ISBN 978-0-12-547612-6, San Diego, USA

Price, C.J.; Wang, D.; Menon, D.K.; Guadagno, J.V.; Cleij, M.; Fryer, T.; Aigbirhio, F.; Baron, J.C. & Warburton, E.A. (2006). Intrinsic Activated Microglia Map to the Peri-Infarct Zone in the Subacute Phase of Ischemic Stroke. *Stroke*, Vol.37, No.7, (July 2010), pp. 1749-1753, ISSN 1524-4628

Rausch, M.; Hiestand, P.; Baumann, D.; Cannet, C. & Rudin, M. (2003). MRI-Based Monitoring of Inflammation and Tissue Damage in Acute and Chronic Relapsing EAE. *Magnetic Resonance in Medicine,* Vol.50, No.2, (February 2003), pp. 309-314, ISSN 07403194

Rojas, S.; Martin, A.; Arranz, M.J.; Pareto, D.; Purroy, J.; Verdaguer, E.; Llop, J.; Gomez, V.; Gispert, J.D.; Millan, O.; Chamorro, A. & Planas, A.M. (2007). Imaging Brain Inflammation with [C-11]Pk11195 by PET and Induction of the Peripheral-Type Benzodiazepine Receptor After Transient Focal Ischemia in Rats. *Journal of Cerebral Blood Flow and Metabolism,* Vol.27, No.12, (December 2007), pp. 1975-1986, ISSN 0271-678X

Song, P.J.; Barc, C.; Arlicot, N.; Guilloteau, D.; Bernard, S.; Sarradin, P.; Chalon, S.; Garreau, L.; Kung, H.F.; Lantier, F. & Vergote, J. (2010). Evaluation of Prion Deposits and Microglial Activation in Scrapie-Infected Mice Using Molecular Imaging Probes. *Molecular Imaging and Biology,* Vol.12, No.6, (December 2010), pp. 576-582, ISSN 1860-2002

Steinbrecher, A.; Weber, T.; Neubergeru, T.; Mueller, A.M.; Pedre, X.; Giegerich, G.; Bogdahn, U.; Jakob, P.; Haase, A. & Faber, C. (2005). Experimental Autoimmune Encephalomyelitis in the Rat Spinal Cord: Lesion Detection with High-Resolution MR Microscopy at 17.6 T. *AJNR American Journal of Neuroradiology,* Vol.26, No.1, (January 2005), pp. 19-25, ISSN 0195-6108

Stephenson, D.T.; Schober, D.A.; Smalstig, E.B.; Mincy, R.E.; Gehlert, D.R. & Clemens, J.A. (1995). Peripheral Benzodiazepine Receptors are Colocalized with Activated Microglia Following Transient Global Forebrain Ischemia in the Rat. *Journal of Neuroscience,* Vol.15, No.7, (July 1995), pp. 5263-5274, ISSN 0270-6474

Sugama, S.; Cho, B.P.; Baker, H.; Joh, T.H.; Lucero, J. & Conti, B. (2002). Neurons of the Superior Nucleus of the Medial Habenula and Ependymal Cells Express IL-18 in Rat CNS. *Brain Research*, Vol.958, No.1 (January 2002), pp. 1-9, ISSN 0006-8993

Takano, A.; Arakawa, R.; Ito, H.; Tateno, A.; Takahashi, H.; Matsumoto, R.; Okubo, Y. & Suhara, T. (2010). Peripheral Benzodiazepine Receptors in Patients with Chronic Schizophrenia: a PET Study with C-11 DAA1106. *International Journal of Neuropsychopharmacology*, Vol.13, No.7, (August 2010), pp. 943-950, ISSN 1461-1457

Venneti, S.; Lopresti, B.J. & Wiley, C.A. (2006). The Peripheral Benzodiazepine Receptor (Translocator Protein 18 kDa) in Microglia: From Pathology to Imaging. *Progress in Neurobiology*, Vol.80, No.6 (December 2006), pp. 308-322, ISSN 0301-0082

Venneti, S.; Wang, G.J.; Nguyen, J. & Wiley, C.A. (2008). The Positron Emission Tomography Ligand DAA1106 Binds with High Affinity to Activated Microglia in Human Neurological Disorders. *Journal of Neuropathology and Experimental Neurology,* Vol.67, No.10 (October 2008), pp. 1001-1010, ISSN 0022-3069

Vowinckel, E.; Reutens, D.; Becher, B.; Verge, G.; Evans, A.; Owens, T. & Antel, J.P. (1997). PK11195 Binding to the Peripheral Benzodiazepine Receptor as a Marker of Microglia Activation in Multiple Sclerosis and Experimental Autoimmune Encephalomyelitis. *Journal of Neuroscience Research*, Vol.50, No.2 (October 1997), pp. 345-353, ISSN 0360-4012

Willenborg, D.O.; Sjollema, P. & Danta, G. (1986). Immunoregulation of Passively Induced Allergic Encephalomyelitis. *Journal of Immunology,* Vol.136, No.5, (March 1986) pp. 1676-1679, ISSN 0022-1767